RSC Advances

Accepted Manuscript

This article can be cited before page numbers have been issued, to do this please use: V. M. Sharma, D. Saha, G. Madras and T. Guru Row, *RSC Adv.*, 2013, DOI: 10.1039/C3RA43518K.

View Article Online
DOI: 10.1039/C3RA43518K

Graphical abstract

Synthesis, structure, characterization and photocatalytic activity of $Bi_2Zr_2O_7$ under solar radiation

Vaishali Sharma M, Dipankar Saha, Giridhar Madras*, T. N. Guru Row*

Solid State and Structural Chemistry Unit, Indian Institute of Science, Bangalore 560 012, India.

$Bi_2Zr_2O_7$, synthesized via solution combustion method using two fuels, exhibited good photocatalytic activity that was attributed to the oxygen vacancy.

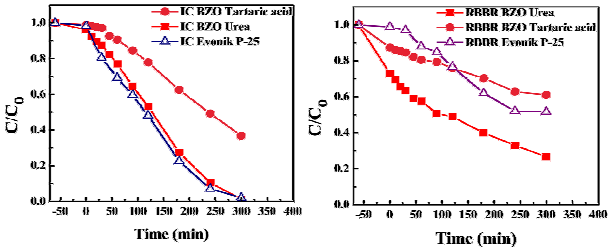

View Article Online
DOI: 10.1039/C3RA43518K

Synthesis, structure, characterization and photocatalytic activity of $Bi_2Zr_2O_7$ under solar radiation

Vaishali Sharma M, Dipankar Saha, Giridhar Madras*, T. N. Guru Row*

Solid State and Structural Chemistry Unit, Indian Institute of Science,

Bangalore 560 012, India.

Address for correspondence

* Professor Giridhar Madras,

Solid State and Structural Chemistry Unit,

Indian Institute of Science,

Bangalore-560 012, INDIA

Tel: +91-80-22932321

Fax: +91-80-23608121

E-mail: giridhar@chemeng.iisc.ernet.in

* Professor T. N. Guru Row,

Solid State and Structural Chemistry Unit,

Indian Institute of Science,

Bangalore-560 012, INDIA

Tel: +91-80-2292796

Fax: +91-80-3601310

E-mail: ssctng@sscu.iisc.ernet.in

View Article Online
DOI: 10.1039/C3RA43518K

Abstract

$Bi_2Zr_2O_7$ was synthesized via facile solution combustion method. Two different fuels, urea and tartaric acid were used in synthesis, which resulted in $Bi_2Zr_2O_7$ with different band gaps and surface areas. The structure has been determined by Rietveld refinement followed by difference Fourier technique. The compound crystallizes in the space group $Fm\ \bar{3}\ m$. The photocatalytic degradation of two dyes was carried out under solar radiation. $Bi_2Zr_2O_7$ prepared using urea as the fuel exhibits higher photocatalytic activity than the compound prepared using tartaric acid and comparable to that of commercial Evonik P-25 TiO_2. This is traced to be due to the oxygen vacancy occurring in the two cases, urea based compound has an occupancy of 0.216, whereas the tartaric acid based synthesis shows a disorder in the oxygen position amounting to a small amount of oxygen vacancy.

Keywords: Solution combustion; Photodegradation; Rietveld refinement; Difference Fourier map.

View Article Online
DOI: 10.1039/C3RA43518K

1. Introduction

Bismuth oxide has drawn attention for its various applications in industry, particularly in the area of catalysis and fuel cells. Bi_2O_3 exhibits polymorphism with four different crystallographic forms. [1-4] The low temperature α form crystallizes in the space group $P2_1/c$ with cell parameter a = 5.8496(3) Å, b = 8.1648(4) Å, c = 7.5101(4) Å, β = 112.977(3)˚. The monoclinic polymorph transforms to face-centered cubic δ form (Space group $Fm\bar{3}m$ a = 5.6595(4) Å) at 729°C, which is stable up to the melting point at 824°C. On cooling, either of the metastable polymorph i.e. tetragonal β (a = 7.741(3) Å and c = 5.634(2) Å, space group $P\square42_1c$) or body-centered cubic γ (a = 10.268(1) Å, space group $I23$) can be obtained. The β phase appears at 650°C while the γ phase appears at 639°C. The formation of the metastable phase depends on small amounts of impurities. [2-4] On cooling, the β-phase transforms to the α-phase at 303°C and the γ-phase at 500°C, although the γ-phase may persist at room temperature with slow cooling rates. [2-4]

The high temperature δ-Bi_2O_3 is best known as an oxide ion conductor and is an appealing material for practical purposes such as a solid electrolyte in galvanic cells or in an oxygen sensor. Therefore, efforts have been made to stabilize the δ-Bi_2O_3 at room temperature by substitutions at Bi site. [5-9] Cation size plays an important role in stabilizing the FCC phase. It was found that smaller rare earth ions were more effective in stabilising the δ-phase at room temperature.[10] The use of rare earth ions as dopant to stabilize bismuth oxide at room temperature has been reviewed. [11] The solid state system Bi_2O_3:ZrO_2 has also been investigated towards the stabilization of δ-Bi_2O_3. Compounds having general formula $Bi_{2-x}Zr_xO_{3-x/2}$ ($0.05 \leq x \geq 0.17$) were found to adopt β-Bi_2O_3 type structure. [12] Hund reported a tetragonal phase for $Zr_{1-x}Bi_xO_{2-x/2}$ compositions prepared at 800°C where x ranged from 0.3 to 1.0.0. [13] It is of

View Article Online
DOI: 10.1039/C3RA43518K

interest to note that the study by Sorokina and Sleight revealed that $Bi_2Zr_2O_7$ crystallizes in a defect fluorite phase. [14] However, the oxygen position in these systems has raised controversy. [15-17] Though several bismuth based compounds has been used for photocatalysis, the Bi-Zr based compounds have shown higher potential for photocatalytic activity [18] and hence the structure determination becomes crucial to explain the reasons for the enhanced photocatalytic activity.

In this article, we report the synthesis of $Bi_2Zr_2O_7$ (BZO) via a facile solution combustion method and structure determination by using a unique approach of combining Rietveld refinement with difference Fourier analysis. This methodology clearly establishes that the structure adopts cubic Fcc δ-Bi_2O_3 with oxygen partially occupying the 32*f* Wyckoff position. The compound prepared using urea as the fuel (BZOU) and the compound prepared using tartaric acid (BZOT) displays an oxygen disorder. The photocatalytic activity under solar radiation have been characterized and explained with respect to the structural features.

2. Experimental

2.1. Synthesis of $Bi_2Zr_2O_7$ (BZO)

BZO was synthesized by the solution combustion method. Solution combustion is a self propagating, high temperature, single step synthesis method. [19] This method is simple and effective in obtaining crystalline materials with different morphology and particle size. [20]

In the synthesis of BZO by the solution combustion method, three fuels namely urea, tartaric acid and glycine were used; $Bi(NO_3)_3.6H_2O$ and $ZrO(NO_3)_2.H_2O$ were taken as the precursors. Initially, $Bi(NO_3)_3.6H_2O$ was dissolved in 5 M nitric acid to make a clear solution and $ZrO(NO_3)_2.H_2O$ was dissolved in double distilled water. Both were mixed in a petri dish, stirred with a magnetic stirrer and a stoichiometric amount of fuel was added. Urea, glycine and

View Article Online
DOI: 10.1039/C3RA43518K

tartaric acid were used as the fuel, which was added to clear solution and the resultant mixture was kept in preheated furnace maintained at 500°C. The heat that is produced when fuel undergoes combustion is absorbed by the precursor, which then accelerates the chemical reaction. [16] After the combustion reaction, the final product was kept in the furnace maintained at 500°C for 5 h to obtain pure BZO. The resultant mixture was yellow pale in color. The X-ray diffraction patterns are shown in Fig. 1. The diffraction data from BZO prepared using urea (BZOU) and tartaric acid (BZOT) indicates the formation of pure compound, while BZO prepared using glycine (BZOG) has impurity peaks. The impurity peaks in BZOG, were identified as Bi_2O_3 (reference code: 00-050-1088), ZrO_2 (reference code: 00-024-1164) and $Bi_{1.75}Zr_{0.25}O_3$ (reference code: 04-011-0960) using profile fitting method (JANA 2000). [21] (Fig. S1, see electronic supporting information). BZOG was discarded from further experiments due to these impurities. The approximate crystallite size of BZOU and BZOT were determined using the Scherrer's formula based on the 28.52 ° peak to be 4 - 5 nm and 3 - 4 nm, respectively.

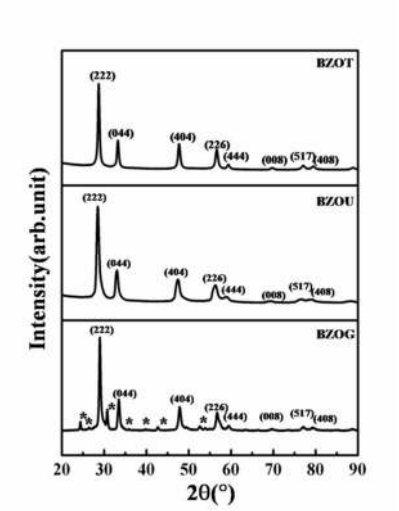

Fig. 1 X- ray powder diffraction of pure phase BZOT, BZOU and BZOG. * indicates impurity peaks.

View Article Online
DOI: 10.1039/C3RA43518K

The chemical with urea and tartaric acid as fuel proceeds as follows

$$2Bi(NO_3)_3.6H_2O + 2ZrO(NO_3)_2.H_2O + CH_4N_2O \longrightarrow Bi_2Zr_2O_7 + CO_2 + 6N_2 + 16H_2O + 11O_2$$

$$2Bi(NO_3)_3.6H_2O + 2ZrO(NO_3)_2H_2O + C_4H_6O_6 \longrightarrow Bi_2Zr_2O_7 + 4CO_2 + 5N_2 + 17H_2O + 12O_2$$

2.2. Sample characterization

FET Quanta scanning electron microscopy and TEM were used for morphological analysis of BZO compound. Band gap of the materials were determined by UV-vis diffuse reflectance spectra which was recorded on Perkin Elmer Lambda 35 UV-vis spectrophotometer. Surface area was determined by BET analysis using porosimeter (Belsorp, Japan). Rietveld quality data was obtained after the confirmation of phase purity using X -pert diffractometer with Cu Kα radiation over the angular range of $5° \leq 2\theta \leq 105°$, with step size 0.008° with exposure time of 450 s.

2.3. Photodegradation experiments

The degradation of cationic dye such as Ramazoline brilliant blue (RBBR) and anionic dye such as Indigo carmine (IC) in the presence of BZO and Evonik P-25 was carried out simultaneously to ensure similar exposure to solar radiation. The experiment was conducted between 10 a.m. and 3 p.m. when solar intensity fluctuation were minimal. The average solar intensity during this period was 800 W m^{-2}. The degradation was carried out for the same catalyst loading of 1 g/L. Photodegradation of both anionic dye and cationic dye in the presence of BZO and Evonik P-25 under solar radiation was studied. The dye was dissolved in double distilled Millipore filtered water and taken in 250 ml cylindrical borosilicate glass beaker

View Article Online
DOI: 10.1039/C3RA43518K

(diameter 6 cm, height 9 cm) covered with watch glass. To ensure that the degradation is due to the catalyst, solutions were stirred for 1 h prior to the solar experiment so that we can account the change in dye concentration due to adsorption. Less than 5% adsorption was observed in case of IC and 27% adsorption was observed in case of RBBR. The solution was stirred continuously and exposed to solar radiation. Samples were collected at regular time intervals and the supernatant was centrifuged for 30 min prior to the analysis. UV-vis spectrophotometer was used to determine the concentration of the samples. The λ_{max} used for the measurement was 611 nm and 593 nm for IC and RBBR, respectively.

3. Result and discussions

3.1. Characterization

Fig. 2 shows the results from microscopic studies on BZOU and BZOT. Selected area diffraction pattern (SAED) was used to confirm the crystalline nature of the sample. SEM micrographs show no significant changes in the morphology BET analysis reveal that the surface area and mean pore diameter to be 1.2 m^2/g, 15.7 nm and 2.3 m^2/g, 42.4 nm for BZOU and BZOT, respectively. Fig. 3 (a) shows the diffused reflectance spectra for the compounds and Fig 3 (b) provides the Tauc plot. Using the Kubelka-Munk function [$F(R) = (1 - R)^2/2R$], where R is reflectance, the band gap for BZOU and BZOT is estimated to be 2.6 eV and 2.9 eV respectively. These band gap values suggest that both compounds may be suitable for visible light photocatalysis. The slope of the edge in the Tauc plot of BZOU is low indicating the presence of vacancies. The valence band energy in each case calculated as $E_{VB} = X - E_e + 0.5\ E_g$ where E_e is the energy of free electron on the hydrogen scale, X is the electronegativity of the compound expressed as the geometrical mean of the absolute electronegativity of the constituent

View Article Online
DOI: 10.1039/C3RA43518K

atoms,[22] is 2.7 eV and 2.8 eV for BZOU and BZOT. The corresponding E_{cb} values are +0.1 eV and -0.1 eV. Because E_{vb} is above the oxidation potential to form OH radical, photo degradation proceeds with the formation of photo generated holes. The oxygen vacancy thus prevents the recombination by trapping the electron and hence enhances the photodegradation process.[18] Rietveld refinements carried out on both the compounds indicate the presence of oxygen vacancy. In BZOU, the occupancy of the oxygen position refines to a value of 0.219 while in case of BZOT the oxygen position is disordered with total occupancy of 0.294. This oxygen vacancy, which results in a positively charged site can act as electron capturing centers and thus reduce the recombination of charges, which in turn is responsible for the photodegradation of dye.

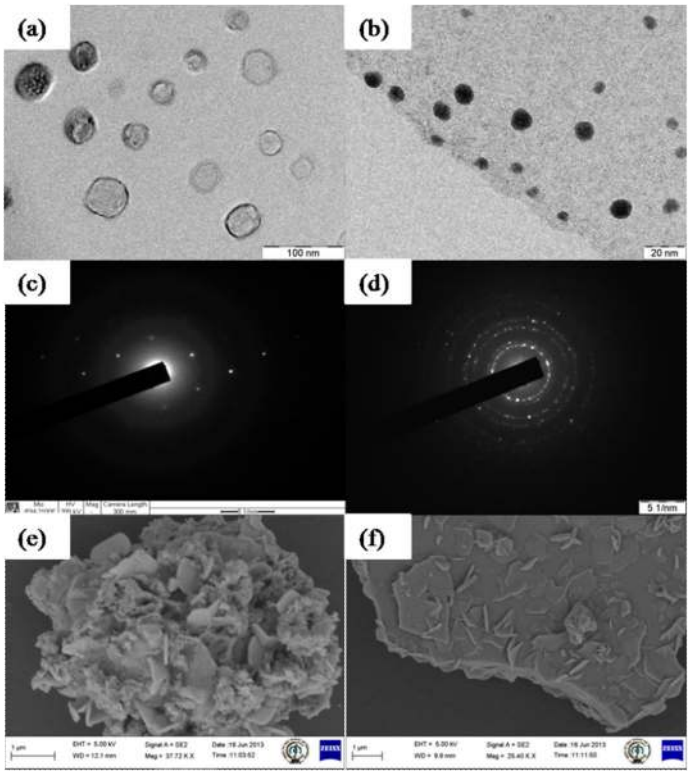

Fig. 2 (a)-(b) TEM image, (c)-(d) SAED and (e)-(f) SEM micrograph of BZOU and BZOT respectively.

View Article Online
DOI: 10.1039/C3RA43518K

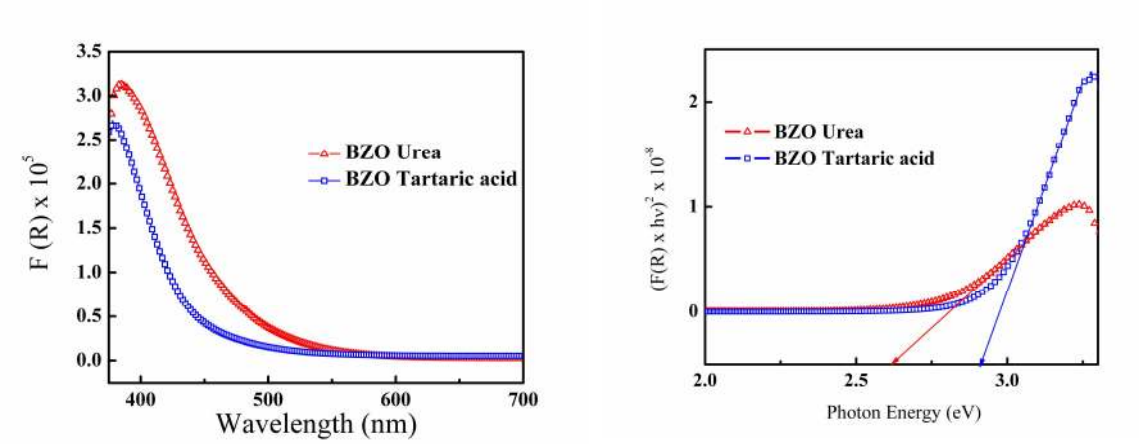

(a) (b)

Fig. 3 (a) Diffuse reflectance spectra and (b) Tauc plot of BZOU and BZOT respectively

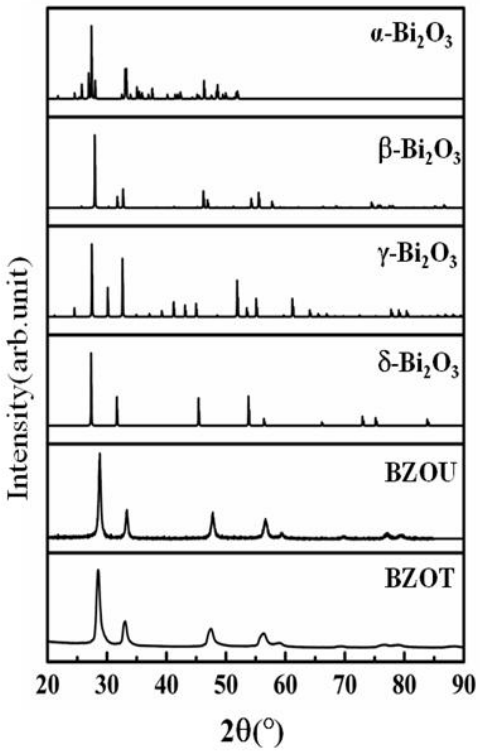

Fig. 4 Comparison of simulated powder pattern of different polymorphs of Bi_2O_3 and $Bi_2Zr_2O_7$.

View Article Online
DOI: 10.1039/C3RA43518K

3.2. Structure from Powder X-ray diffraction

Pure phase of BZO was obtained via solution combustion using tartaric acid and urea as fuels. The phase prepared using these two different fuels showed identical powder pattern, as shown in Fig. 1. The crystal structure of a BZOU and BZOT was refined using high resolution X-ray diffraction data. Fig. 4 shows a comparison between the $Bi_2Zr_2O_7$ and simulated powder patterns of different polymorphs of Bi_2O_3 .[2-3] It is found that the PXRD pattern of BZOU and BZOT match with that of δ-FCC cubic form of Bi_2O_3 with shifts in 2θ positions, which is due to the substitution of smaller Zr^{4+} cation at the Bi^{3+} site. Therefore, δ-FCC cubic form of Bi_2O_3 was chosen as a starting model.

Bismuth in δ- Bi_2O_3 is positioned in 4 *a* and several models has been proposed to explain the oxygen position, the earliest is Gattow and Schrőder [15] where the oxygen atom is positioned in 8*c* site with an average occupancy of 75% with random distribution of vacancies. The model due to Battle *et al.* [16] has the oxygen atom occupying both at 8*c* and 32*f* sites with partial occupancy. The starting model for our compound was taken from the model proposed by Harwig, [17] where oxygen atom is at was in 32 *f* [(*x x x*) *x* = 0.316(2)] with an initial occupancy of 0.5. The powder pattern obtained for both BZOU and BZOT were indexed with a = 5.6595(4) Å in the space group $Fm\bar{3}\ m$ profile refinements using JANA 2000 [21] were carried out to confirm the space group and the cell dimension obtained (Fig. S2, see electronic supporting information). Rietveld refinement were then carried out based on Harwig [17] model with the inclusion of Zr in Bi position with both Bi and Zr sharing 50:50 occupancy. Fig. 5 (a) shows the fitted profile after Rietveld refinement in case of BZOU with final R-factor for the fitted model being 0.042. Based on difference Fourier map calculated (Figure 6 (a)), Wyckoff position 32 *f* [(*x x x*) *x* = 0.308(1)] was assigned to the oxygen atom and its occupancy further refined to 0.219(2) in case of BZOU.

View Article Online
DOI: 10.1039/C3RA43518K

Fig. 5(b) shows the fitted profile after Rietveld refinement and the final R-factor for the fitted model was 0.0517 for BZOT. It is of interest to note that the oxygen atom is disordered at two positions as found from the difference Fourier map (Fig.6 (c-e)), one occupying the Wycoff position 32 *f* [(*x x x*) *x* = 0.308(1)] with its refined occupancy value of 0.203(2) and the other at the Wycoff position 4 *b* (0.5 0.5 0.5) with refined occupancy value of 0.091(3). It is to be pointed out that the final fit has still some unaccounted asymmetry in the profile in case of BZOT, which could be a consequence the uncertainty associated with the disordered oxygen position. These structural difference in BZOU and BZOT correlated with the photocatalytic behavior as described later.

The refined parameters are listed in table 1 and featureless difference electron density maps in both cases indicate the correctness of the model.

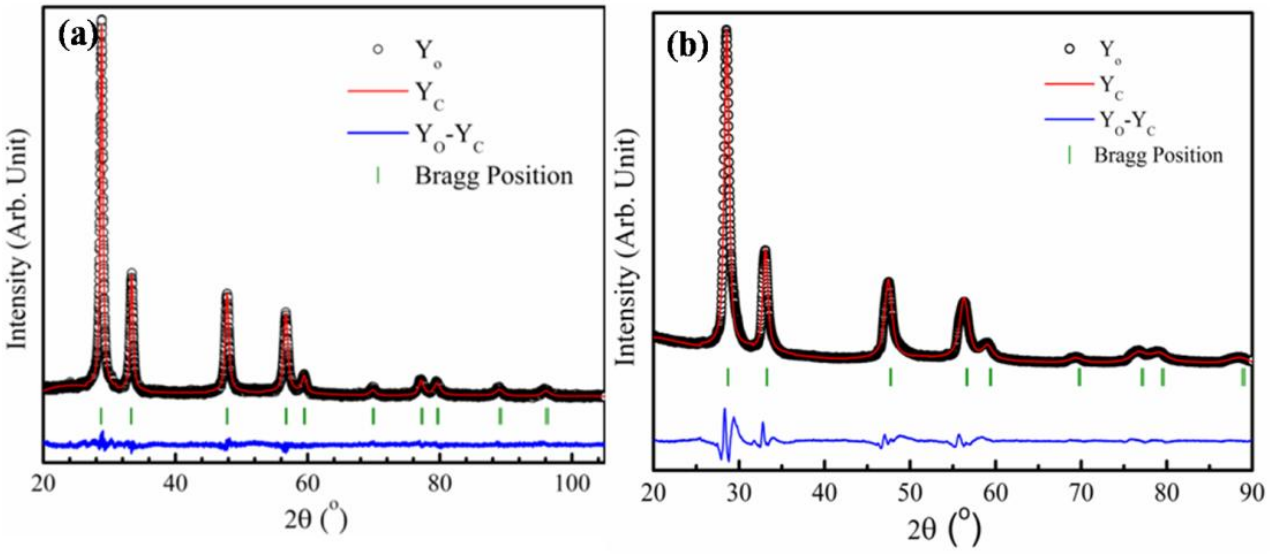

Fig. 5 Fitted profile for (a) BZOU and (b) BZOT after Rietveld refinement.

View Article Online
DOI: 10.1039/C3RA43518K

Table 1. Crystallographic parameters after Rietveld refinement.

Empirical Formula	$Bi_2Zr_2O_7$ (BZOU)	$Bi_2Zr_2O_7$ (BZOT)
Formula weight	713.08	713.08
Wavelength(Å)	1.5418	1.5418
Space group	*Fm* $\bar{3}$ *m*	*Fm* $\bar{3}$ *m*
a (Å)	5.38463(6)	5.3916(2)
Volume/Å^3	156.123(6)	156.728(18)
Z	1	1
Density/g cm^{-3}	7.578	7.554
R_p,	0.0422	0.0517
R_{wp}	0.0552	0.0765
DWd	1.002	0.033
χ^2	1.040	37.72

View Article Online
DOI: 10.1039/C3RA43518K

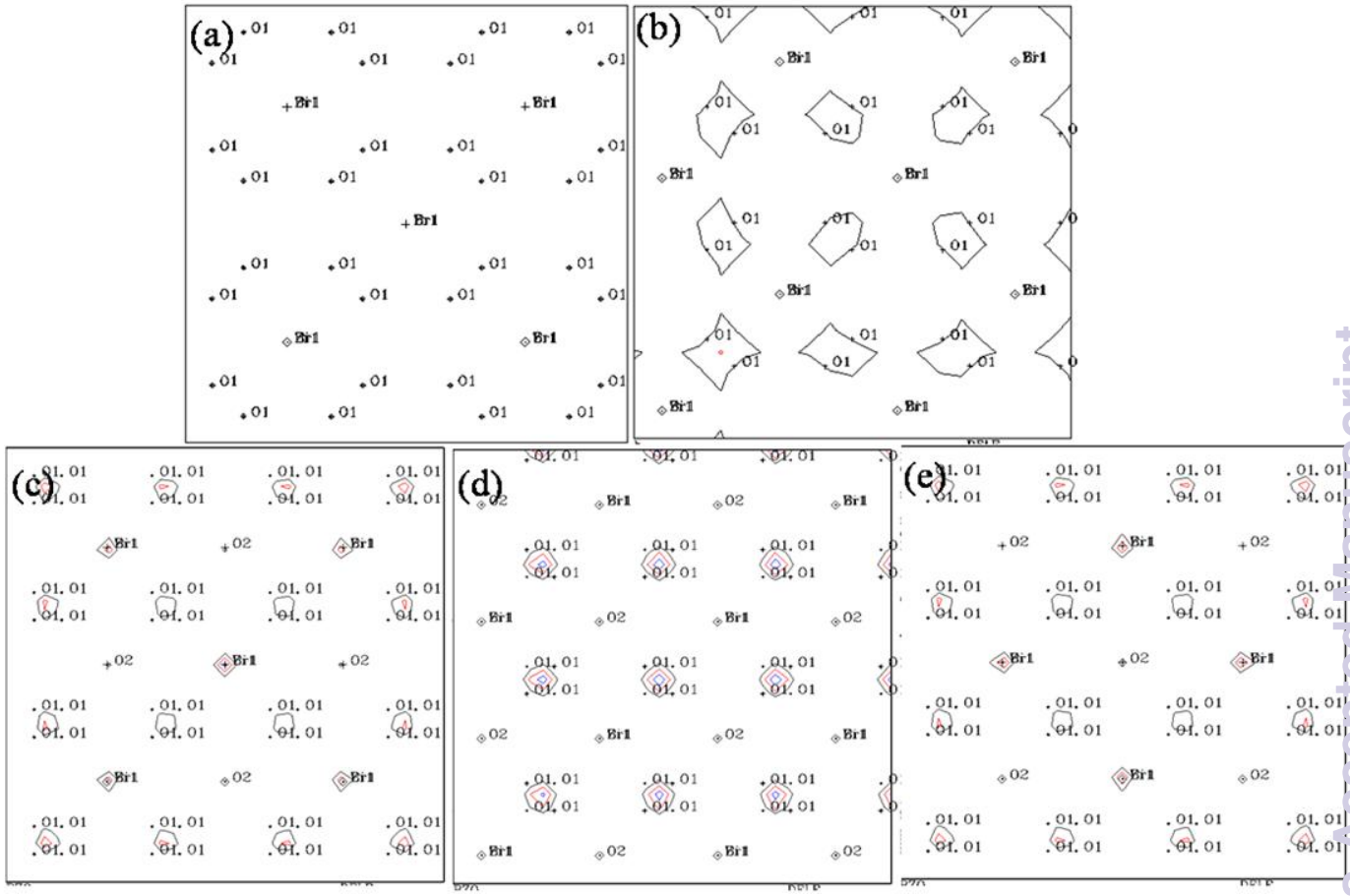

Fig. 6 Difference Fourier map of (a-b) BZOU and (c-e) BZOT based on our model

3.3. Photocatalysis

The degradation profile of RBBR dye is shown in Fig. 7. This clearly shows that BZOU has higher photocatalytic activity than BZOT and is comparable to Evonik P-25. Fig. 8 shows the degradation profile of Indigo carmine (IC). The complete degradation of IC is observed when BZOU is used as the catalyst and the degradation profile again is comparable with that observed with Evonik P-25. However, only 60 % degradation was observed in IC when BZOT compound was used.

View Article Online
DOI: 10.1039/C3RA43518K

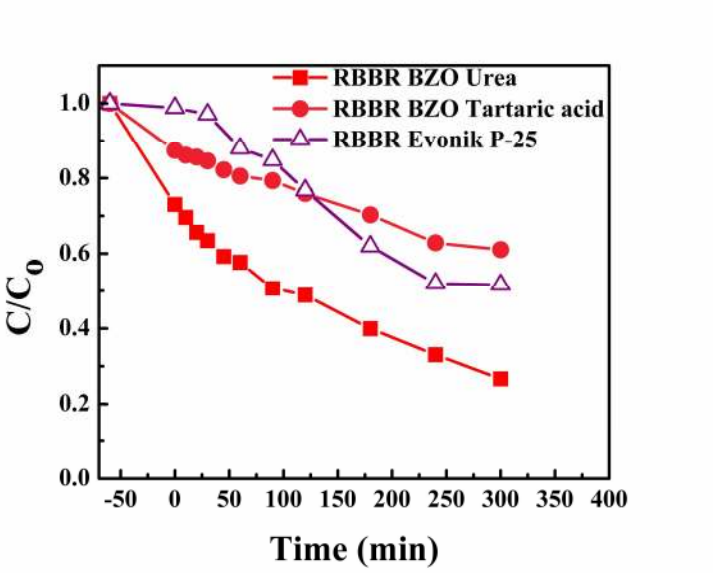

Fig. 7 Degradation profile of RBBR under solar radiation in presence of BZOU, BZOT and Evonik P-25.

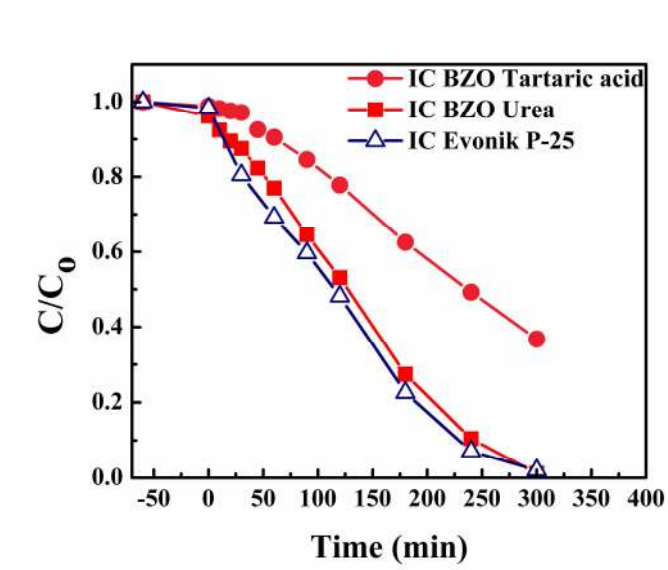

Fig. 8 Degradation profile IC under solar radiation in presence of BZOU, BZOT and Evonik P-25.

View Article Online
DOI: 10.1039/C3RA43518K

The higher activity of BZOU could be traced to lower band gap (2.6 eV) when urea is used as a fuel compared to the case where tartaric acid is used as fuel (2.9 eV). This lowering in band gap generally helps in easy formation of electrons and holes. It is to be noted that higher oxygen vacancy in BZOU appears to aid in the reduction of the band gap and hence influence higher catalytic activity.

The valence band of the compound is not favorable for $OH^{\bullet}$ formation and the photodegradation of dye is due to the generated holes. [24] The oxygen vacancy in these materials act as electron trapping centers, reducing the recombination of holes and electron and thus enhancing the degradation rate.

4. Conclusions

Pure phase of $Bi_2Zr_2O_7$ compound was prepared via solution combustion method using urea and tartaric acid as fuels. Characterization of both the compounds has been done by SEM and TEM. Rietveld refinement has been done and it is confirmed that it crystallizes in $F\,m\bar{3}\,m$ space group. Oxygen position was determined using Difference Fourier maps and correctness of our model was supported by the featureless electron density map. During this, it was confirmed that the BZOT was having disordered oxygen position with lower oxygen vacancy compared to BZOU. This structural difference resulted in difference in photocatalytic activity. The surface areas of BZOU and BZOT were less than 2.5 m^2/g and the band gap was determined to be 2.6 eV and 2.9 eV, respectively. Based on this, photodegradation of anionic dye were carried out under solar light. BZOU showed comparable photocatalytic activity with respect to Evonik P-25 TiO_2.

View Article Online
DOI: 10.1039/C3RA43518K

Acknowledgements

We acknowledge the funding from DST, India and financial support for the XRD machine from the DST-FIST program. T. N. G. thanks DST-India for a J. C. Bose fellowship for funding. Author thanks IISc for JRF and Mr. Jarali for BET measurement.

References

1 W.C. Schumb and E.S. Rittner, *J. Am. Chem. Soc.*, 1943, **65**, 1055-1060.

2 H.A. Harwig and A.G. Gerards, *Thermochim. Acta*, 1979, **28**, 121-131.

3 H.A. Harwig, *Z. Anorg. Allg. Chem.*, 1978, **444**, 151-166.

4 H.A. Harwig and J.W. Weenk, *Z. Anorg. Allg. Chem.*, 1978, **444**, 167-177.

5 T. Takahashi and H. Iwahara, *Mater. Res. Bull.*, 1978, **13**, 1447-1453.

6 M. Thompson and C. Greaves, *Solid State Ionics*, 2010, **181**, 1674-1679.

7 M. Thompson, T. Herranz, B. Santos, J.F. Marco, F.J. Berry and C. Greaves, *J. Solid State Chem.*, 2010, **183**, 1985-1991.

8 N. Jiang, E.D. Wachsman and S.-H. Jung, *Solid State Ionics*, 2002, **150**, 347-353.

9 G. Gattow and H. Schröder, *Z. Anorg. Allg. Chem.*, 1962, **318**, 176-189.

10 H. Iwahara, T. Esaka, T. Sato and T. Takahashi, *J. Solid State Chem.*, 1981, **39**, 173-180.

11 N.M. Sammes, G.A. Tompsett, H. Näfe and F. Aldinger, *J. Eur. Ceram. Soc.*, 1999, **19**, 1801-1826.

12 I. Abrahams, S.C.M. Chan, F. Krok and W. Wrobel, *J. Mater. Chem.*, 2001, **11**, 1715-1721.

13 F. Hund, *Z. Anorg. Allg. Chem.*, 1964, **333**, 248-255.

14 S.L. Sorokina and A.W. Sleight, *Mater. Res. Bull.*, 1998, **33**, 1077-1081

View Article Online
DOI: 10.1039/C3RA43518K

15 G. Gattow and D. Schütze, *Z. Anorg. Allg. Chem.*, 1964, **328**, 44-68.

16 P.D. Battle, C.R.A. Catlow, J. Drennan and A.D. Murray, *J. Phys. C: Solid State Phys.*, 1983, **16**, L561-L566.

17 Harwig, H. A.; Gerards, A. G. *J. Solid State Chem.* **26** (1978) 265.

18 Z. Zhang, W. Wang, E. Gao, M. Shang and J. Xu, *J. Hazard. Mater.,*2011, **196**, 225-262

19 K.C. Patil, M.S. Hegde, T. Rattan, S.T. Aruna, *Chemistry of Nanocrystalline Oxide Materials: Combustion Synthesis, Properties and Applications*, World Scientific, New Jersey 2008.

20 M.S.Hegde, G.Madras, K.C.Patil, *Acc.Chem.Res*., 2009, **42**, 704-712.

21 V. Petricek, M. Dusek and L. Palatinus, Jana2000, 08/11/2007 ed., 2007

22 M. L. Guan, D. K. Ma, S. W. Hu, Y. J. Chen and S. M. Huang, *Inorg. Chem.*, **2011**, 50, 800-805

23 D. Saha, G. Madras and T.N.G. Row, *Dalton Trans.*, 2012, **41**, 9598-9600.

24 R. Vinu and G. Madras, *J.Indian Inst.Sci*., 2010, **90**, 189-230.